

Multi-core parallel tempering Bayeslands for basin and landscape evolution

Rohitash Chandra^{b,a}, R. Dietmar Müller^{1,c}, Ratneel Deo^b, Nathaniel Butterworth^c, Tristan Salles^a, Sally Cripps^{b,d}

^aEarthByte Group, School of Geosciences, University of Sydney, NSW 2006, Sydney, Australia

^bCentre for Translational Data Science, University of Sydney, NSW 2006, Sydney, Australia

^cSydney Informatics Hub, University of Sydney, NSW 2006, Sydney, Australia

^dSchool of Mathematics and Statistics, University of Sydney, NSW 2006
Sydney, Australia

Abstract

In recent years, Bayesian inference has become a popular methodology for the estimation and uncertainty quantification of parameters in geological and geophysical forward models. Badlands is a basin and landscape evolution forward model for simulating topography evolution at a large range of spatial and time scales. Previously, Bayesian inference has been used for parameter estimation and uncertainty quantification in Badlands, an extension known as Bayeslands. It was demonstrated that the posterior surface of these parameters could exhibit highly irregular features such as multi-modality and discontinuities making standard Markov Chain Monte Carlo (MCMC) sampling difficult. Parallel tempering (PT) is an advanced MCMC method suited for irregular and multi-modal distributions. Moreover, PT is more suitable for multi-core implementations that can speed up computationally expensive geophysical models. In this paper, we present a multi-core PT algorithm implemented in a high performance computing architecture for enhancing Bayeslands. The results show that PT in Bayeslands not only reduces the computation time over a multi-core architecture, but also provides a means to improve the sampling process in a multi-modal landscape. This motivates its usage in larger-scale problems in basin and landscape evolution models.

Keywords: Landscape evolution, Bayesian inference, Parallel tempering, Badlands, Bayeslands

1. Introduction

Recent developments in Earth evolution models have the capability to link models for dynamic and isostatic topography through time [1] with landscape evolution models [2]. This has given the opportunity to model landscape evolution in response to surface uplift and subsidence over a large range of spatial scales, and track sediments from source to sink [3, 4]. Geophysical forward models depend on uncertain initial and boundary conditions [5], but a large variety of observations are available to optimise and ground-truth these models. Uncertain input parameters for these models include time-dependent topography, relative sea level change, time-varying rainfall and rock lithology and erodibility [6, 7]. Observations useful for model ground-truthing include digital elevation models and river geometries, sediment thickness and stratigraphy in sedimentary basins, and other geological proxies for landscape evolution.

Bayesian inference provides a rigorous approach for uncertainty quantification [8, 9, 10] and emerged as a popular tool for fitting complex parameter models to data [11]. This provides advantages over optimization methods that provide single point solutions and need multiple experimental runs for uncertainty quantification [12, 13]. Estimation of parameters that fit observational data in geophysical models have shifted from optimization [14] to inference that addresses uncertainty quantifi-

cation given that the models provide an approximation of geophysical processes [15]. Markov Chain Monte Carlo (MCMC) sampling methods implement Bayesian inference where a sample of the desired distribution is obtained by observing the chain after a number of steps [16, 17, 18, 19]. Bayesian methods have become popular in geophysics in the past few decades [20, 21, 22, 23]. The convergence in canonical MCMC sampling methods face further challenges when the size of the problem increases in terms of the number of parameters and computational time of running the model. This is a challenge in geophysics that use forward models such as Badlands [3, 4]. Although advanced MCMC methods such as Hamiltonian based samplers have been proposed [24, 25, 26], they require gradient information from the models to form proposals. Acquiring gradient information from complex geo-physical models such as Badlands is difficult, therefore, Bayesian inference via MCMC random-walk proposals was proposed in a framework called Bayeslands [27]. Bayeslands demonstrated that the posterior surface of selected parameters could exhibit highly irregular features, such as multi-modality and discontinuities which made it difficult for sampling. Hence, there is a need to explore efficient sampling methods that feature gradient free proposals and addresses multi-modality.

Parallel tempering [28, 29] is a MCMC sampling scheme designed for sampling multi-modal distributions. Another feature is their feasibility of implementation in multi-core or parallel computing architectures. Due to massive computational requirements of geo-physical models, parallel computing archi-

Email address: rohitash.chandra@sydney.edu.au (Rohitash Chandra)

tectures have been widely utilized in geosciences [30, 31, 32]. This can therefore help us to extend and improve our previous approach called Bayeslands that featured Bayesian inferences via MCMC random-walk sampler for Badlands [27]. Hence, the major limitations such as computational time and the need for efficient multi-modal distribution given by the MCMC random-walk sampler in Bayeslands can be overcome by multi-core parallel tempering.

In this paper, we present a multi-core parallel tempering approach for Bayeslands that features uncertainty quantification and estimation of selected parameters for basin and landscape evolution. We use selected problems that feature synthetic and real-world applications for selected parameters such as rainfall and erodibility that affect the topography development over thousands of years. We evaluate the performance of multi-core parallel tempering Bayeslands (PT-Bayeslands) for selected number of multiprocessing cores and report the overall computation time. The results report the successive predicted topographies, successive sediments given by erosion-deposition, their prediction accuracy, posterior distribution of selected parameters for selected problem, and also the overall computation time.

The rest of the paper is organised as follows. Section 2 provides a background on Badlands and Bayeslands. Section 3 presents the methodology and Section 4 presents the experiments and results. Section 5 provides a discussion and Section 6 concludes the paper with directions for future research.

2. Background and Related Work

2.1. Badlands

Over the last decades, many numerical models have been proposed to simulate how the Earth surface has evolved over geological time scales in response to different driving forces such as tectonics or climatic variability [33, 34, 35, 36, 37]. These models combine empirical data and conceptual methods into a set of mathematical equations that can be used to reconstruct landscape evolution and associated sediment fluxes [38, 39]. They are currently used in many research fields such as hydrology, soil erosion, hillslope stability and general landscape studies.

In this paper, we use *Badlands* [3, 40, 41]. This framework is intended to simulate regional to continental sediment deposition and associated sedimentary basin architecture [4, 42]. In its most simple formulation, the Earth surface elevation change is related to the interaction of three types of processes, one driven by tectonic, another describing the smoothing effects associated to diffusive processes, and a last one representing the erosive power of water flow:

$$\frac{\partial z}{\partial t} = -\nabla \cdot \mathbf{q}_s + u$$

where u in $m \cdot yr^{-1}$ is a source term that represents tectonic uplift. The total downhill sediment flux \mathbf{q}_s is defined by:

$$\mathbf{q}_s = \mathbf{q}_r + \mathbf{q}_d$$

\mathbf{q}_s is the depth-integrated, bulk volumetric soil flux per width ($m^2 \cdot yr^{-1}$). \mathbf{q}_r represents transport by fluvial system and \mathbf{q}_d hillslope processes.

Here the fluvial incision is based on the classical detachment-limited stream power law (SPL), in which erosion rate $\dot{\epsilon}$ depends on drainage area A , net precipitation P and local slope S and takes the form:

$$\dot{\epsilon} = \kappa(PA)^m S^n$$

κ is an erodibility coefficient while m and n are positive exponents characterising the contribution of rain and slope respectively on erosion processes. Despite its simplicity, the SPL reproduces many of the characteristic features of natural systems where detachment-limited erosion regime dominates [33]. With this formulation, sediment deposition occurs solely in topographically closed depression and marine offshore regions. Constraining the exact values of κ , m and n from natural landscapes is relatively complex and not easily measured from direct field observations. Their values depend on the geomorphological, climatic and tectonic context and their ranges are commonly admitted to be:

- $0 < m < 2$
- $0 < n < 4$
- κ varies by several orders of magnitude not only based on lithology, climate, sedimentary flux or river channel width but also with the chosen values of m and n .

In addition to overland flow, semi-continuous processes of soil displacement are accounted for using a linear diffusion law commonly referred to as soil creep [34]:

$$\frac{\partial z}{\partial t} = \kappa_d \nabla^2 z$$

in which z is the elevation and κ_d is the diffusion coefficient. This transport rate depends linearly on topographic gradient and encapsulates in a simple formulation the processes operating on superficial sedimentary layers.

2.2. Bayeslands

Bayeslands [27] illustrates how Bayesian inference, via the posterior distribution, can be used to estimate and quantify the uncertainty surrounding initial conditions of factors such as rainfall and erodibility. Formally, given some data, \mathbf{D} , we make inference regarding unknown parameters, denoted by θ , via the posterior distribution $p(\theta|\mathbf{D})$, given by Bayes rule,

$$p(\theta|\mathbf{D}) = \frac{p(\mathbf{D}|\theta)p(\theta)}{P(\mathbf{D})}$$

where $p(\mathbf{D}|\theta)$ is the likelihood of the data given the parameters, $p(\theta)$ is the prior, and $P(\mathbf{D})$ is a normalizing constant and equal to $\int p(\mathbf{D}|\theta)p(\theta)d\theta$. Frequently the posterior distribution does not have a closed form solution and it is approximated by a sampling based estimate.

Bayeslands used MCMC to obtain samples of θ from the posterior distribution by proposing values from some known distribution $q(\theta)$. The value of θ is then set equal to these proposed values with a probability which ensures the detailed balance condition is met, otherwise the chain remains in its current position, see [43]. The transition kernel which moves the Markov chain from one point to another in the parameter space is the product of the proposal distribution q and the acceptance probability. Under certain conditions, the draws from this transition kernel converge to draws from the stationary distribution, $p(\theta|\mathbf{D})$. This algorithm is known as the Metropolis-Hastings (MH) algorithm [16] which is given in Algorithm 1

Alg. 1 Metropolis-Hastings (MH)

Result: Drawing from $p(\theta|\mathbf{D})$

Set maximum number of iterations, K , and initialize $\theta = \theta^{[0]}$

Set the current value of θ , $\theta^c = \theta^{[0]}$

for $k = 1, \dots, K$ **do**

1. Propose a new value of θ , $\theta^p \sim q(\theta|\theta^c)$

2. Compute acceptance probability

$$\alpha = \min\left(1, \frac{p(\theta^p|\mathbf{D})q(\theta^c|\theta^p)}{p(\theta^c|\mathbf{D})q(\theta^p|\theta^c)}\right)$$

3. Draw $u \sim U[0, 1]$

if $u < \alpha$ **then**

| $\theta^{[k]} = \theta^p$

else

| $\theta^{[k]} = \theta^c$

end

end

The development of transitions kernels which efficiently explore posterior distributions has been the subject of much research in sampling methods [24]. Bayeslands has major limitations since MCMC random-walk requires thousands of samples to accurately explore the posterior distribution. Executing it in a sequential manner that employs only one processing unit becomes a computational challenge taking into account the time needed to run Badlands when the application problem covers a larger region featuring millions of years. We will address these computational challenges using multi-core parallel tempering in this paper.

2.3. Parallel tempering

Posterior distributions of parameters in geophysical inversions problems are notoriously difficult to explore. They are high dimensional, multi-modal and very irregular, by which we mean the derivative of posterior is often difficult to compute and/or it has many discontinuities. An example is shown in Figure 1 that features the likelihood surface of the Continental Margin problem used in Bayeslands [27]. While proposal

distributions based on canonical random-walk MCMC methods are gradient free, in sampling multi-modal posterior distributions, they become very inefficient [44]. As evident, the likelihood surface can be highly multi-modal and irregular which makes it natural for these algorithms to be trapped in a local minimum. In such situations, proposal distributions that feature gradients such as Hamiltonian methods will also face difficulties since there are local convergence issues related to gradient based methods [45]. In complex geophysical inversion problems, proposal distributions usually need to gradient free and explore most, if not all the posterior modes. Methods such as gradient-free Hamiltonian Monte-Carlo [46] do not address highly irregular and complex multi-modal distributions.

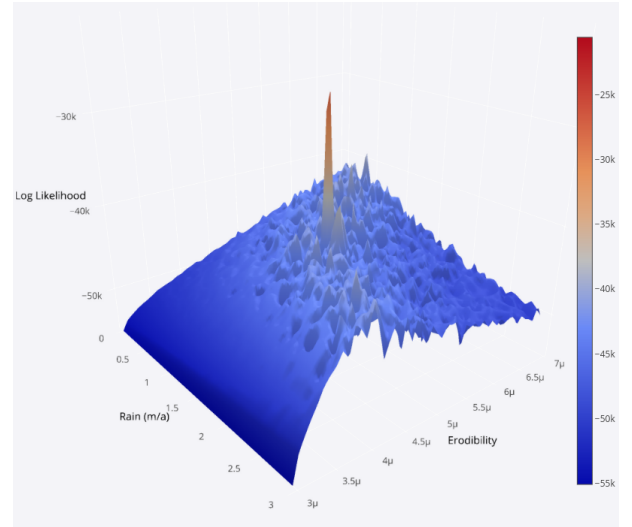


Figure 1: Likelihood surfaces of the Continental Margin topography for the rainfall and erodibility parameters only[27].

Parallel tempering has been motivated by thermodynamics of physical systems where the temperature of a system determines the ability to change [47]. Parallel tempering is also known as replica exchange or the Multi-Markov Chain method [48, 49] suitable for multi-modal distributions by running multiple MCMC chains at different *temperatures* in parallel. Typically, gradient free proposals within chains are used for proposals for exploring multi-modal and discontinuous posteriors [50, 51].

The Markov chains in the parallel replicas have stationary distributions which are equal to (up to a proportionality constant) $p(\theta|\mathbf{D})^\beta$, where $\beta \in [0, 1]$, with $\beta = 0$ corresponds to a stationary distribution which is uniform and $\beta = 1$ corresponds to a stationary distribution which is the posterior. The replica with smaller values of β are able to explore a larger regions of distribution, while those with higher values of β typically explore local regions.

Communication between the parallel replicas is essential for the efficient exploration of the posterior distribution. This is done by considering the chain and the parameters as part of the space to be explored as highlighted in Algorithm 2. Suppose there are M chains, indexed by m , with corresponding stationary distributions, $p_m(\theta|\mathbf{D}) = p(\theta|\mathbf{D})^{\beta_m}$, for, $m = 1, \dots, M$, with

$\beta_1 = 1$ and $\beta_M < \beta_{M-1} < \dots, \beta_1$, then the pair (m, θ) are jointly proposed and accepted/rejected according to the MH algorithm. The stationary distribution of this sampler is proportional to $p(\theta|\mathbf{D})^{\beta_m} p(m)$. The quantity $p(m)$ must be chosen by the user and is referred to as a *pseudo-prior*. For efficient mixing of the chain we use $q(m^p = m^c \pm 1|m^c) = 1/2$, for $1 < m^c < M$, and $q(m^p = m^c + 1|m^c = 1) = q(m^p = m^c - 1|m^c = M) = 1$.

Alg. 2 Metropolis-Hastings Parallel Tempering (MHPT)

Result: Drawing from $p(\theta|\mathbf{D})$

Set maximum number of iterations, K , and initialize $\theta = \theta^{[0]}$, and $m = m^{[0]}$

Set the current value of θ , to $\theta^c = \theta^{[0]}$ and m to $m^c = m^{[0]}$

for $k = 1, \dots, M$ **do**

1. Update $\theta^{[k]}$, from the chain with $p(\theta|\mathbf{D})^{\beta_{m^c}}$ as its invariant distribution according to Alg 1.
2. Propose a new value of m^p , from $q(m^p|m^c)$.
3. Compute acceptance probability

$$\alpha = \min\left(1, \frac{p(\theta^{[k]}|\mathbf{D})^{\beta_{m^p}} p(m^p) q(m^c|m^p)}{p(\theta^{[k]}|\mathbf{D})^{\beta_{m^c}} p(m^c) q(m^p|m^c)}\right)$$

4. Draw $u \sim U[0, 1]$

if $u < \alpha$ **then**

 | $m^{[k]} = m^p$

else

 | $m^{[k]} = m^c$

end

end

A number of attempts have been made to improve the parallel tempering algorithm, which includes the efficient way of finding β_m for $m = 1, \dots, M$, [52, 47], exchange of solutions among the replicas [53], and joint adaption β_m and the proposal distributions for θ in the corresponding chain, [54]. The potential for parallel tempering in geoscience problems has been demonstrated [55] with examples that better convergence than conventional approaches for complex multi-modal optimization problems [50, 51, 14]. A number of factors need to be considered in multi-core implementation which specifically takes into account operating system concepts such as interprocess communications when considering exchange of solutions between the chains [56]. In order to address this, a decentralized implementation of parallel tempering was presented that eliminates global synchronization and reduces the overhead caused by interprocess communication in exchange of solutions between the chains that run in parallel cores [57]. Parallel tempering has also been implemented in a distributed volunteer computing network where computers belonging to the general public are used with help of multi-threading and graphic processing units (GPUs) [58]. Furthermore, parallel tempering has been implemented with Field Programmable Gate Arrays (FPGAs) that has massive parallelizing capabilities which showed much better performance than multi-core and GPU implementations

[59]. Furthermore, in terms of applications, other studies have efficiently implemented parallel tempering via multi-core architectures for exploration of Earth's resources [60].

3. Methodology: Multi-Core Parallel Tempering Bayeslands

The task of sampling or running geophysical models is computationally intensive, it is worthwhile to employ parallel computing approach to parallel tempering since thousands of samples are required for efficiently sampling a posterior distribution. Massive parallelizing in multi-core architectures that implements the various chains of the parallel tempering sampling method can help in speeding up the approach while exploring multi-modal posterior distributions. Furthermore, Parallel tempering being a method for implementing Bayesian inference naturally accounts for uncertainty quantification. Therefore, we present a multi-core parallel tempering approach for addressing the limitations of Bayeslands. The overall problem remains the same as Bayeslands, where the task is in sampling from the posterior distribution of selected parameters such as rainfall and erodibility that contribute to the topography development over time with Badlands. In doing so, it is essential to define the likelihood function that will be used to determine where the proposals are accepted.

The remainder of the section defines the model that features the likelihood and priors for parallel tempering Bayeslands. Furthermore, the generation of systematic topographies for the selected problems and the details of implementation of multi-core parallel tempering for Bayeslands is also given.

3.1. Model and Priors

The likelihood function essentially captures the quality to the proposals by considering the difference between the simulated final topography and the actual one. In the problems where sediment deposition occurs, the likelihood function also considers the difference between the simulated and real successive topographies at selected time intervals.

Let the initial topography be denoted by \mathbf{D}_0 , with $\mathbf{D}_0 = (D_{0,s_1} \dots, D_{0,s_n})$, where s_i corresponds to site s_i , with coordinates latitude, u_i , and longitude, v_i . Suppose that we are interested in the topography t years into the future, we will denote this by \mathbf{D}_t , with \mathbf{D}_T defined to be the current topography. Our model for the process which generates the topography is

$$D_{t,s_i} = f_{t,s_i}(\boldsymbol{\theta}) + \epsilon_{t,s_i} \text{ with } \epsilon_{t,s_i} \sim (0, \tau^2) \quad (1)$$

for $t = 0, 1, \dots, T$ and $i = 1, \dots, n$, where $\boldsymbol{\theta}$ are the parameters of the Badlands model and $f_{t,s_i}(\boldsymbol{\theta})$ is the output of the Badlands forward model. This model states that the topography is function of the Badlands forward model given parameters $\boldsymbol{\theta}$, plus some Gaussian noise with zero mean and variance τ^2 . The likelihood function $L_t(\boldsymbol{\theta})$, is given by

$$L_t(\boldsymbol{\theta}) = \frac{1}{(2\pi\tau^2)^{n/2}} \exp\left\{-\frac{1}{2} \frac{\sum_{t=1}^T \sum_{i=1}^n (D_{t,s_i} - f_{t,s_i}(\boldsymbol{\theta}))^2}{\tau^2}\right\}$$

where the subscript l , in $L_l(\theta)$, denotes that it is the landscape likelihood.

Although it may be possible to observe previous topologies, it is not likely and therefore we assume that only the current topology \mathbf{D}_T is available. However it may be possible to observe other landscape features of the past, such as sediment deposits, and we wish to incorporate the information contained in this data to constrain landscape evolution. We allow for this possibility by defining another random variable $\mathbf{z}_t = (z_{t,s_1}, \dots, z_{t,s_m})$ which are the sediment deposits at sites s_1, \dots, s_m . We assume that observed values of \mathbf{z}_t are a function of the Badlands forward model, with parameter θ and some Gaussian noise

$$z_{t,s_i} = g_{t,s_i}(\theta) + \eta_{t,s_i} \text{ with } \eta_{t,s_i} \sim (0, \sigma^2) \quad (2)$$

then the sediment likelihood, $L_s(\theta)$ is

$$L_s(\theta) = \frac{1}{(2\pi\sigma^2)^{mT/2}} \exp \left\{ -\frac{1}{2} \sum_{t=1}^T \sum_{j=1}^m \frac{(Z_{t,s_j} - g_{t,s_j}(\theta))^2}{\sigma^2} \right\}$$

giving a total likelihood as a function of theta $L(\theta)$ to be

$$L(\theta) = L_s(\theta) \times L_l(\theta).$$

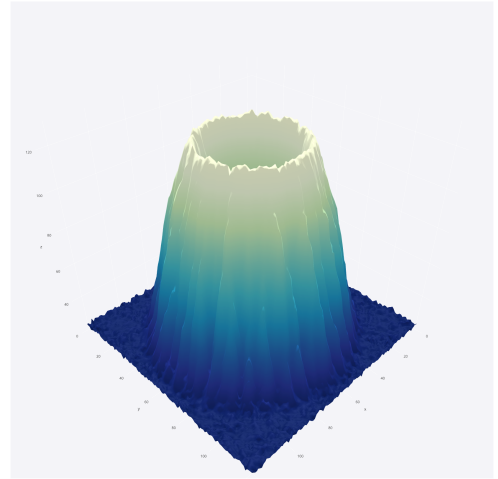
The prior distribution, also known as prior, refers to one's belief in the distribution of the parameter without taking into account the evidence or data [61]. The prior distribution is adjusted by sampling from the posterior with given likelihood function that takes into account the data and the model. In the case of the priors for Bayeslands, we focus on a subset of the parameters of the Badlands model depending upon the problem, see Table tab:truevalues. The complete set of unknowns in our model is θ , τ^2 and σ^2 . We follow the setup in [27] and place uniform priors on the unknown parameters with limits given in Table 3.

3.2. Synthetic topography data

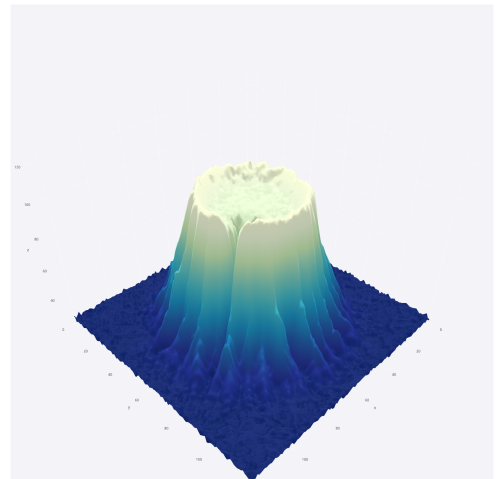
Badlands is a forward stratigraphic model that requires an initial topography and values for θ to simulate an expected final (ground-truth) topography at time T , given by $\mathbf{f}_T(\theta)$ in equation 1, and expected sediment deposits at several points in time, given by $g_{t,s_i}(\theta)$ using Equation 2.

We consider five landscape problems from which two are taken from Bayeslands which consist of a crater and continental margin (CM) example, where only two parameters (rainfall and erodibility) are sampled. In this work, we present two variants of these problems, such as crater-extended and CM-extended. The extended problems consider additional parameters and simulation time for topography development. Furthermore, we also use a mountain building case that features uplift rates as a parameter which is not present in the other problems. The initial topographies for the crater-extended and CM-extended cases appear in Figure 2 and Figure 3, respectively. The final topography after 50,000 years and 1,000,000 years along with erosion-deposition is also given. The Crater and CM cases have an initial and ground-truth topography identical to

[27]. Figure 4 shows the initial and ground-truth final topography of the Mountain landscape problem after 1,000,000 years. Note that there is no erosion-deposition catered for this case in the likelihood function to demonstrate that this data is unavailable. Figure 9 shows the evolution of the PT-Bayeslands model. Tables 2 and 1 shows values of parameters used to create the synthetic ground-truth topography. The parameters for the two crater problems are, rainfall (m/a), erodibility, m-value, and n-value. The CM-extended problem features six free parameters, which include marine diffusion coefficient (c-marine given by m^2/a) and surface diffusion coefficient (c-surface given by m^2/a) as shown in Table 2. The mountain problem features 5 free parameters, rainfall (m/a), erodibility, m-value, and n-value, and uplift (mm/a). The priors were drawn from a uniform distribution with lower and upper limit given in Table 3.



(a) Crater-extended initial topography



(b) Crater-extended synthetic ground-truth topography

Figure 2: Crater-extended: Initial and eroded ground-truth topography and sediment deposition after 50 000 years.

Topography	Evo.(years)	Length [km, pts]	Width [km, pts]	Res. factor	Run-time (s)
Crater [27]	15 000	[0.24, 123]	[0.24, 123]	0.002	0.5
Crater-extended	50 000	[0.24, 123]	[0.24, 123]	0.002	2
CM [27]	500 000	[136.5, 91]	[123.0, 82]	1.5	0.5
CM-extended	1 000 000	[136.0, 136]	[123.0, 123]	1	2.5
Mountain	1 000 000	[80,202]	[40,102]	1	10

Table 1: Landscape evolution problems presented in this paper. The run-time represents the approximate length of time for one model to run.

Topography	Rainfall (m/a)	Erod.	n-value	m-value	c-marine	c-surface	Uplift (mm/a)
Crater [27]	1.5	5.0-e05	1.0	0.5	-	-	-
Crater-extended	1.5	5.0-e05	1.0	0.5	-	-	-
CM [27]	1.5	5.0-e06	1.0	0.5	0.5	0.8	-
CM-extended	1.5	5.0-e06	1.0	0.5	0.5	0.8	-
Mountain	1.5	5.0-e06	1.0	0.5	-	-	1.0

Table 2: True values of parameters

Topography	Rainfall (m/a)	Erod.	n-value	m-value	c-marine	c-surface	uplift
Crater [27]	[0,3.0]	[3.0-e05, 7.0-e05]	-	-	-	-	-
Crater-ext	[0,3.0]	[3.0-e05, 7.0-e05]	[0, 2.0]	[0, 2.0]	-	-	-
CM [27]	[0,3.0]	[3.0-e06, 7.0-e06]	-	-	-	-	-
CM-ext.	[0,3.0]	[3.0-e06, 7.0-e06]	[0, 2.0]	[0, 2.0]	[0.3, 0.7]	[0.6, 1.0]	-
Mountain	[0,3.0]	[3.0-e06, 7.0-e06]	[0, 2.0]	[0, 2.0]	-	-	[0.1, 1.7]

Table 3: Prior distribution range of model parameters

3.3. Multi-core parallel tempering Bayeslands

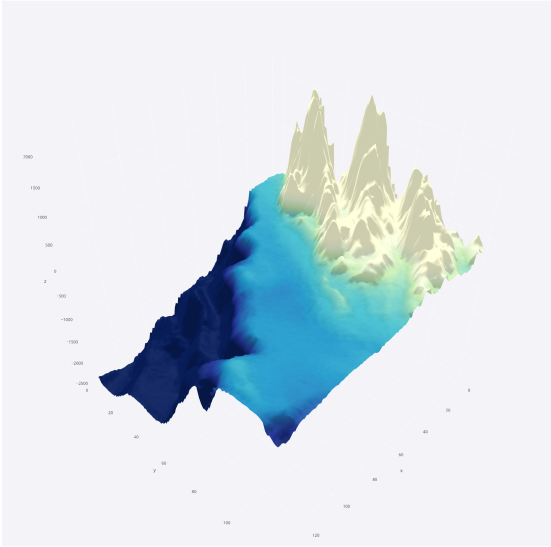
Parallel tempering can be regarded as an ensemble of replicas of a MCMC sampler. Given N replicas in an ensemble defined by multiple temperature levels, the state of the ensemble is specified by $X = \theta_1, \theta_2, \dots, \theta_N$, where θ_i is the replica at temperature level T_i . A Markov chain is constructed to sample θ_i at each temperature level T_i which is used to rescale the likelihood value for the replica in order to give variates in exploration and exploitations during sampling. In other words, . In principle, at every iteration, the Markov chains can feature two types of transitions that include 1) the Metropolis transition and 2) a replica transition. In the *Metropolis transition*, each replica is sampled independently to perform local Monte Carlo moves defined by the temperature which is implemented by a change in the likelihood function for each temperature level T_i .

The *replica transition* considers the exchange of two neighboring replicas that are defined by two neighboring temperature levels, i and $i + 1$, $\theta_i \leftrightarrow \theta_{i+1}$. The exchange is accepted by the Metropolis-Hastings criterion with probability given in Algorithm 2. The exchange enables a replica with a low temperature level to have a chance to reach a high temperature level which gives enhanced exploration features that can enable to escape a local minimum. In this way, the replica exchange can shorten the sampling time required for convergence. The temperature level is user-defined, which needs to be determined from trial experiments, and is highly dependent on the nature of the problem in terms of likelihood surface and multi-modality.

Figure 5 gives an overview of the different replicas that are executed on a multi-processing architecture where each replica runs on a separate core with inter-process communication for

exchanging neighboring replica. The Badlands model is executed in the same processing core where the replicas local sampling is executed. The main process is run on a separate core which controls the replica and enables them to exchange the neighboring replicas given the swap time and probability of exchange is satisfied. In order to minimize interprocess communication between processes for reducing computational costs, we only consider replica transition at fixed intervals that are determined by user defined number of samples used for Metropolis samples. Each replica is allocated a fixed sampling time. The main process waits for all samplers to complete their required sampling after which the samplers attempt configuration exchange. The main process waits for each replica until the swap-interval sampling limit is fulfilled. Once the replica reaches this junction, the main process proposes configuration swaps between adjacent replications depending on the replica exchange probability. The main process notifies the replicas post swapping to resume sampling with latest configurations in the chain for each replica. The process continues with the sampling and proposing swaps until the the maximum sampling time is reached.

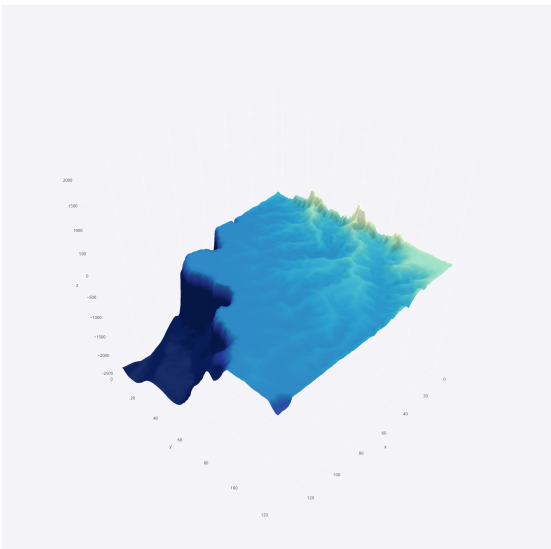
In the multi-core implementation, we need to consider multi-processing software development packages so that the resources have efficient inter-process communication [56] considering the exchange of the solutions between neighboring replica's.



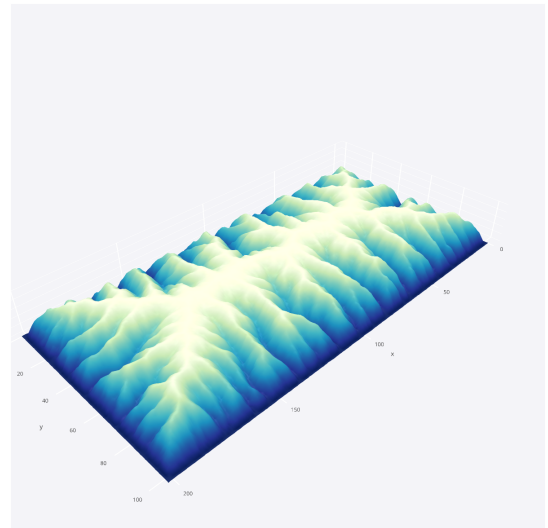
(a) CM-extended initial topography



(a) Mountain initial topography



(b) CM-extended synthetic ground-truth topography



(b) Mountain synthetic ground truth topography

Figure 3: Continental Margin (CM)-extended: Initial and eroded ground-truth topography and sediment after 1 000 000 years.

Figure 4: Mountain: Initial and eroded ground-truth topography after 1 000 000 years evolution.

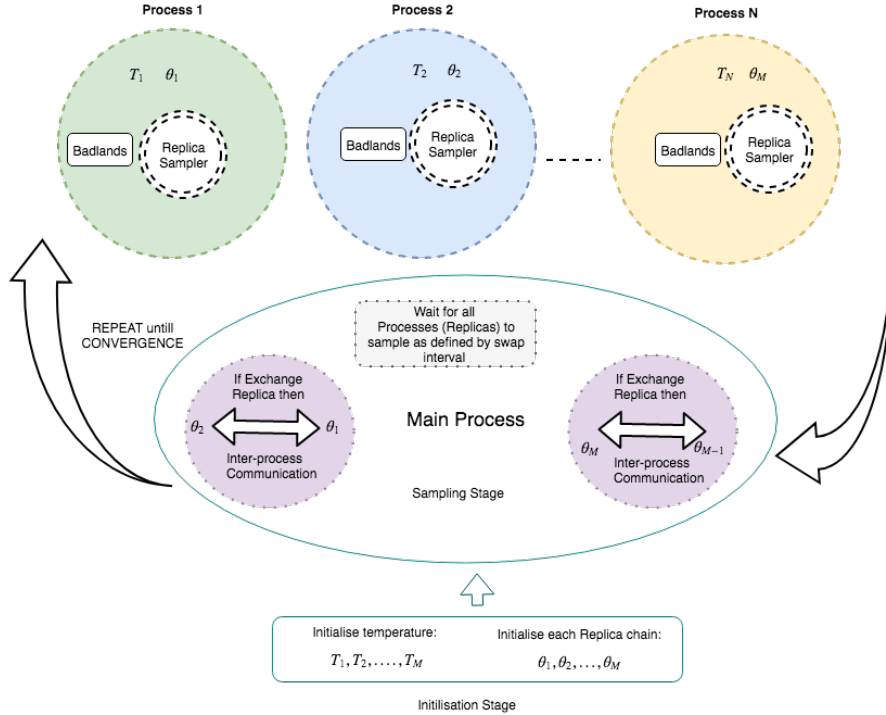


Figure 5: An overview of the different replicas that are executed on a multi-processing architecture. Note that the main process controls the given replicas and enables them to exchange the neighboring replicas given the swap time and probability of exchange is satisfied.

4. Experiments and Results

In this section, we present the experimental design and results for five landscape evolution problems for evaluating the performance of PT-Bayeslands. We use the landscape problems from Table 1, that involve synthetic and real-world topographies. We implemented multi-core parallel tempering using the Python multiprocessing library [62] and open-source software package ¹.

4.1. Design of Experiments

PT-Bayeslands employs a random-walk sampler for each replica chain which is able to run on separate cores (central processing units). The random-walk was implemented by perturbing the chain in the respective replica with a small amount of Gaussian noise with a parameter specific step-size or standard deviation. The step-size β_i for parameter i is chosen to be a combination of a fixed step size $\phi = 0.02$, common to all parameters, multiplied by the range of possible values for parameter i so that

$$\beta_i = (a_i - b_i) * \phi \quad (3)$$

where, a_i and b_i represent the maximum and minimum limits of the priors for parameter and are given in Table 2. Note that PT-Bayeslands samples the parameters with prior distribution

highlighted for the respective problems in Table 3. The step-size ratio ϕ was determined by trial experimental runs that was used by all the problems. Similarly, the temperature change for each of the replica's r was $\delta_r = 2.5$. In trial experiments, the selection of these parameters depended on the prediction accuracy. We used a fix swap ratio, $\eta = 0.1$, that determines when to swap with the neighboring replica which is incorporated into the algorithm 2 and further illustrated in Figure 5. Therefore, the number of samples s required to check when to swap for a given replica r is given as follows.

$$s_r = \eta * (\Phi/\Omega) \quad (4)$$

where Φ is the total number of samples and Ω is the number of replica's for the problem. The experiments are evaluated in terms of total simulation time, acceptance rate of proposals, and root-mean-squared-error (RMSE) of elevation and sediment (Pred. RMSE), which have been defined in the methodology section.

In parallel tempering, the number of replicas needs to be tailored for the problem. They also determine the total simulation time for the problem. It is generally expected that increasing the number of replica's in a multi-core architecture will shorten the computation time; however, additional time is taken with interprocess communication through swapping of neighboring replicas which is also dependent on the swap interval and number of replica's that can contribute to the wait-time by the main process. As shown in Figure 5, the main process runs on a separate core. Therefore given N number of replicas, the total number of processes running will be $N + 1$. The task of the main

¹Parallel tempering Bayeslands: https://github.com/badlands-model/paralleltemp_Bayeslands

process is to manage the ensemble of replicas. It will hold and resume the replica sampling process during the swap period. Moreover, we need to ensure that the quality of the topography and sediment predictions by Badlands is retained when number of cores are increased. Hence, we need to investigate the effect on performance accuracy and time of increasing number of replicas for PT-Bayeslands. The experiments are designed as follows.

- Step 1: Investigate the effects on computational time and accuracy when increasing the number of replicas;
- Step 2: Evaluate the number of samples required for convergence defined in terms of prediction accuracy;
- Step 3: Using knowledge from above experiments, apply PT-Bayeslands to all the given problems and report the posterior distributions, computational time, uncertainty and accuracy in topography and sediment predictions.

We present the crater problem for Step 1 and the CM problem for Step 2. Since the CM problem has demonstrated an irregular multi-modal surface, as shown in Figure 1 [27], it is important to evaluate the effect of sampling time on the posterior distribution and the accuracy of prediction.

4.2. Results

We evaluate the effect of the number of replicas, executed in different cores, has on the total time for the CM-extended topography. Table 4 presents a summary of the results that employs 100,000 samples in PT-Bayeslands for the CM-extended experiment. We observe that increasing the number of replicas reduces the overall computation time. However the number of replicas does not appear to effect the RMSE. Figure 6 shows the effect of the number of cores on the time, panel (a) and on the RMSE, panel (b).

Next, we evaluate the effect of the prediction accuracy given an increase in the number of samples. Table 5 presents summary of the results on the effect of number of samples for the CM-extended topography with 24 replicas. We observe that increasing the number of samples increases the overall time taken, and reduces the acceptance rate of proposals. Moreover, the interval between (10,000 - 100,000) samples does not have a major difference in the prediction accuracy. Hence, even with 10,000 samples, PT-Bayeslands can provide estimation and uncertainty quantification. Due to the stochastic nature of the method and the difficulty of the likelihood surface shown in Figure 1, we don't see a clear trend in convergence when the number of cores (replicas) or samples are increased. The performance depends on initial conditions that is given by the initial points of the chains; depending on how far they are from one of the modes in the likelihood surface, and the tendency to be trapped in a local minimum.

In the next set of experiments, we used 24 cores with 100,000 samples for all the problems. Table 6 shows a summary of results for the given problems. Note that the total prediction accuracy is given by (Pred. RMSE) which consists of sediment

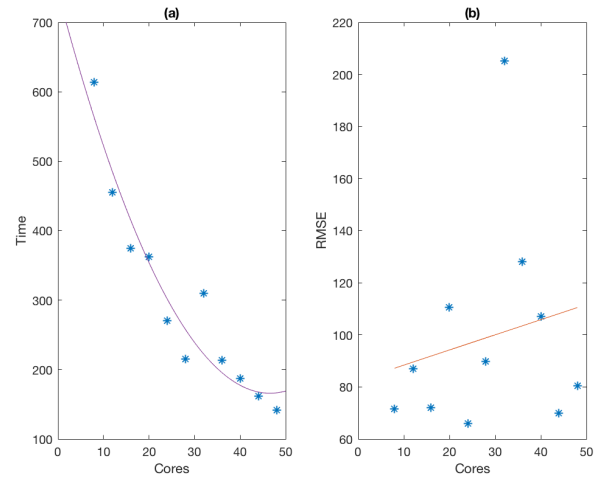


Figure 6: The effect of the number of cores on time, panel (a) and on the RMSE, panel (b). Note that a 95% confidence interval for the slope of the regression line in panel (b), is [-14.2,2.6], showing that the slope is not significantly different from zero.

prediction accuracy (Sed. RMSE) and elevation prediction accuracy (Elev. RMSE). Pred. RMSE considers the difference between the ground-truth and final topography given by Badlands (after maximum number of evolution time in years). However, the Sed. RMSE considers the successive predicted sediments taken equally over 4 different timescales given in years. A major observation here is the overall computation time for the five problems, which is due to the time taken by Badlands to execute each proposal. The crater and crater-extended cases are simpler problems (with shorter evolution time and fewer parameters), hence more proposals are accepted when compared to the CM cases. Moreover, the overall prediction performance (Pred. RMSE) has been significantly improved by PT-Bayeslands. A cross-section of the crater with the uncertainty of prediction is shown in Figure 7.

We select the results for the CM-extended problem from Table 6 and present further details which include; 1.) successive predicted topographies and erosion-deposition at four stages of evolution (Figure 8), 2.) cross-section that gives uncertainty of topography prediction (Figure 10), and 3.) selected posterior distributions, and trace-plots during sampling (Figure 11). Note that erosion is represented as positive while deposition is represented as negative (height in meters) (Figure 8). Posterior distributions, trace plots, and other results for all parameters and all models are available in the on-line supplementary material. In comparison with the true values given in Table 2 that was used to generate the synthetic ground-truth topography, we notice that the true values were not recovered in some of the posterior distributions (e. g. Figure 11). However, as shown in the likelihood surface (Figure 1), a number of sub-optimal values exist. Due to multi-modality, although the true values are not recovered for certain parameters, the sub-optimal modes give accurate predictions. Note that the likelihood surface shown in Figure 1) is for two parameters only (rainfall and erodibility).

Replica (cores)	Time (minutes)	Pred. RMSE	Accepted %
2	3540	78.8	0.1
4	1384	62.7	0.1
8	614	71.5	0.4
12	455	87.0	0.5
16	375	72.0	0.6
20	362	110.6	0.3
24	270	65.9	0.4
28	215	89.7	0.5
32	310	205.1	0.4
36	213	128.0	0.6
40	187	107.0	0.6
44	162	70.0	0.6
48	142	80.5	0.8

Table 4: Effect of number replicas/cores for the CM-extended topography with 100 000 samples.

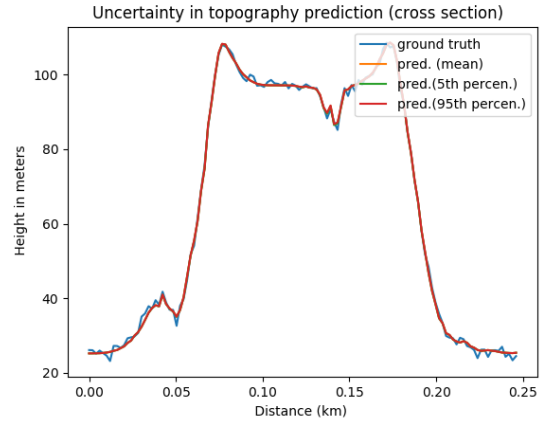


Figure 7: Crater-extended: Cross-section of the elevation along the x-axis comparing the ground-truth of the Badlands-model with the PT-Bayelands predictions.

Comparison with literature (MCMC Bayeslands [27]) is given in Figure 12. The trace-plot in these figures show that the PT-Bayeslands have advantages in exploration with multiple replicas. The comparison of the computational time is given in Table 7. These results show that PT-Bayeslands has a significant improvement in computational time and accuracy in prediction performance.

In this paper, we only show details of the posterior distribution, successive topography and successive erosion-deposition predictions for a sample of model runs. Detailed results for all problems and model runs are provided in supplementary material online ².

5. Discussion

The results have shown that computation time for a given number of iterations does not scale linearly with the number of replicas. There is a trade-off between proposing to swap chains and the rate of convergence of the PT-Bayeslands. Swapping proposals between neighboring replicas, in principle, gives better mixing but introduces computational cost because each chain needs to wait for all the replicas to complete in order to compute the neighbor swap probability. This computational cost can be high if the number of replicas is large. We note that the synthetic problems considered in this paper, only required a few seconds of simulation time for Badlands, whereas, in real-world problems, each simulation of Badlands could take several minutes to hours. In such cases, the trade-off between the frequency of swapping and prediction accuracy would need to be evaluated. In this study, we observed that increasing the number of cores does not necessarily mean that the prediction accuracy will get better. In particular it is advantageous to use a larger number of cores for large scale problems where the Badlands

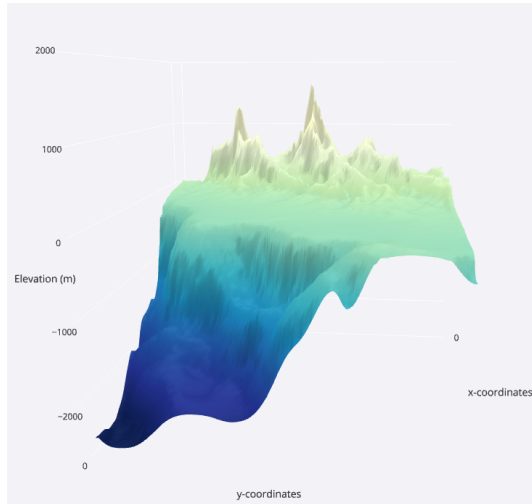
Num. Samples	Time (mins.)	Pred. RMSE	Accepted %
1000	3	120.6	14.0
2000	6	222.5	15.3
4000	10	200.8	9.4
6000	18	98.3	3.7
8000	18	213.1	8.3
10000	27	77.3	2.8
50000	131	77.7	1.3
100000	258	95.1	1.0
150000	436	69.3	0.2

Table 5: Effect of the number of samples for the CM-extended topography running with 24 replicas on 24 cpus.

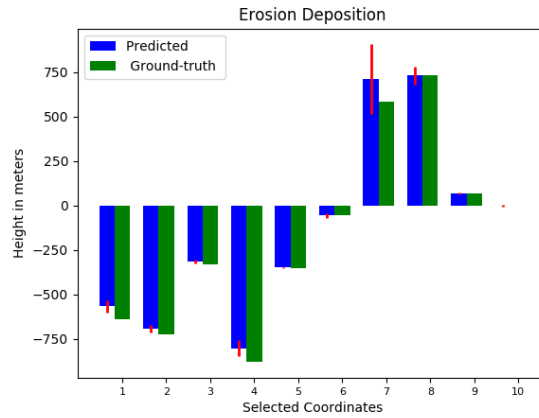
²Supplementary results: https://github.com/badlands-model/paralleltemp_Bayeslands/tree/master/supplementary_results

Topography	Time (minutes)	Sed. RMSE	Elev. RMSE	Pred. RMSE	Accepted %
Crater	80	4.2	1.1	5.3	12.2
Crater-extended	229	0.2	1.0	1.2	1.9
CM	50	2.6	19.9	22.5	1.0
CM-extended	257	50.2	49.0	99.2	0.6
Mountain	375	-	617.0	617.0	0.63

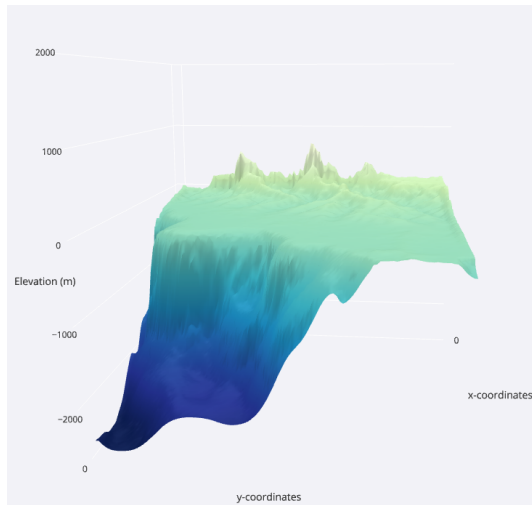
Table 6: Typical results for respective problems (24 replicas/cpus and 100 000 samples). Note that '-' in case of Mountain Sed. RMSE indicates that it was not part of the likelihood function



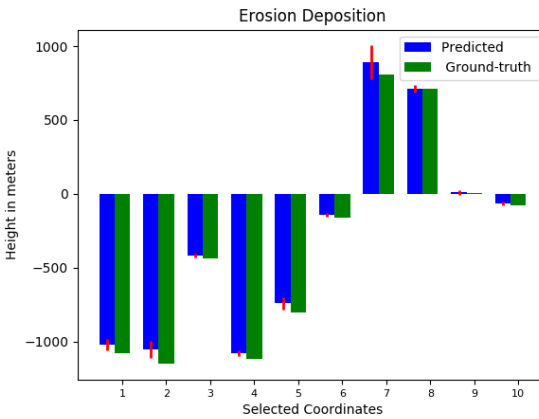
(a) CM-extended predicted topography after 50 % evolution time



(b) CM-extended erosion-deposition after 50 % evolution time



(c) CM-extended predicted topography after 100 % evolution time



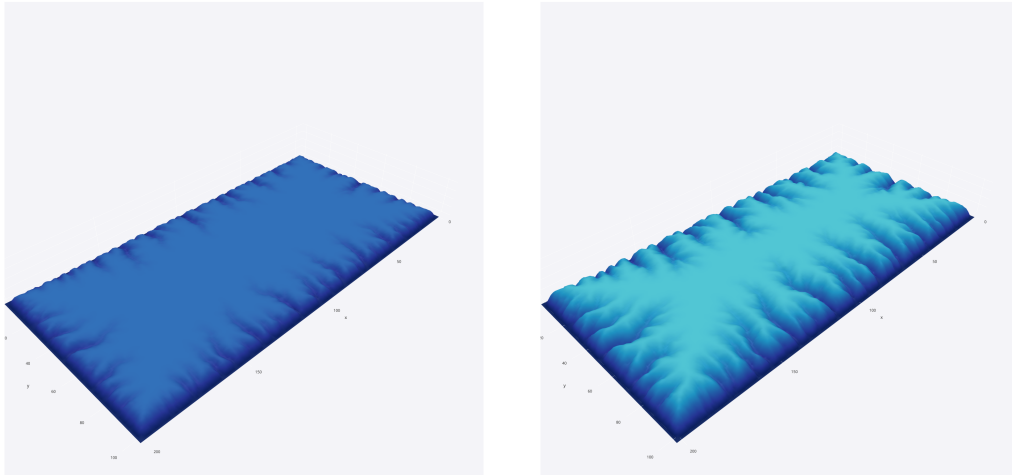
(d) CM-extended erosion-deposition after 100 % evolution time

Figure 8: CM-extended: Topography and erosion-deposition development for selected time frames. Note that erosion (positive) and deposition (negative) values given by the height in meters

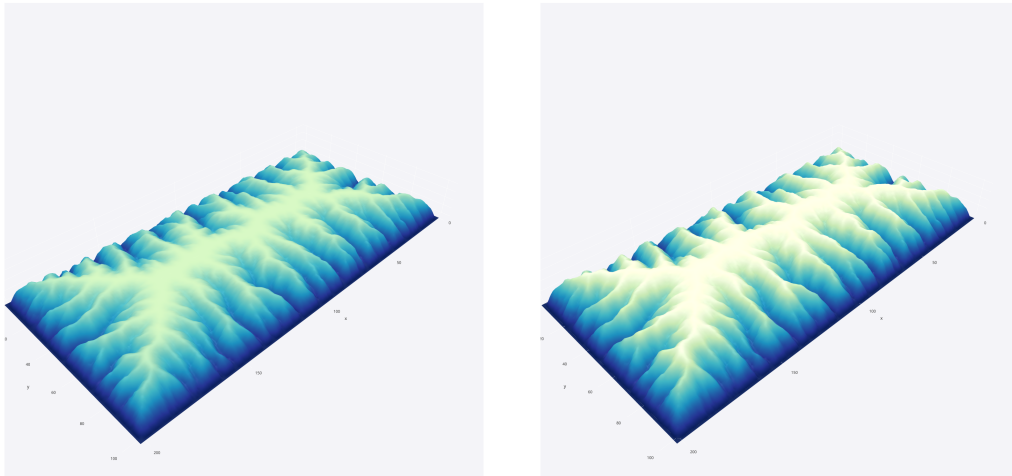
model takes hours to evaluate a single proposal. Moreover, the replica temperature is also an important feature that can be evaluated in future works. Since evaluation of such parameters is computationally expensive for large scale problems, heuristics such as geometric temperature intervals can be used [52, 47].

Figures 12 show the improvement of parallel tempering over

single chain MCMC. Panel (a) in both figures represents output from the single MCMC-Bayeslands while panel (b), represents the output from the PT-Bayeslands. These figures show that PT-Bayeslands mixes more and discovers more of the multiple nodes than the single chain. The degree of improvement of using PT-Bayeslands over single core based MCMC-Bayeslands



(a) Mountain predicted topography after 25 % evolution time (b) Mountain predicted topography after 50 % evolution time



(c) Mountain predicted topography after 75 % evolution time (d) Mountain predicted topography after 100 % evolution time

Figure 9: Mountain evolution over 1 000 000 years.

Topography	Samples	Time(mins)	Sed RMSE	Elev RMSE	Pred RMSE	Accepted%
<i>MCMC Bayeslands results from [27]</i>						
Crater	10,000	136	8.24	1.06	9.30	2.35
Crater	100,000	1023	8.24	1.06	9.30	2.57
CM	10,000	101	459.85	67.37	527.22	0.47
CM	100,000	729	387.92	10.60	398.53	0.02
<i>PT-Bayeslands using 24 replicas (this study)</i>						
Crater	10,000	8	4.2	1.0	5.2	15.0
Crater	100,000	78	4.2	1.1	5.3	12.2
CM	10,000	7	7.4	25.3	32.7	4.9
CM	100,000	50	2.6	19.9	22.5	1.0

Table 7: Comparison of results of PT-Bayeslands with single-threaded MCMC Bayeslands [27] shows significant difference in performance given computational time and accuracy in prediction.

depends upon the type of topography and the parameter. For example, the estimated posteriors distributions for all parameters

in the Crater topography contained the true value of that parameter, while in the CM-extended topography, only some of the

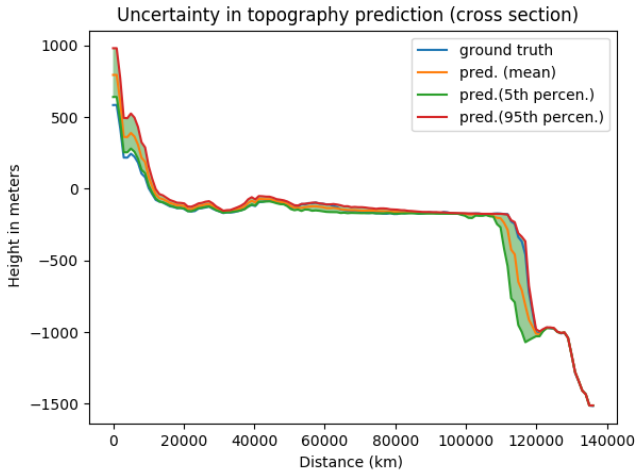


Figure 10: CM-extended: Cross-section of the elevation along the x-axis comparing the ground-truth of the Badlands-model with the PT-Bayelands predictions.

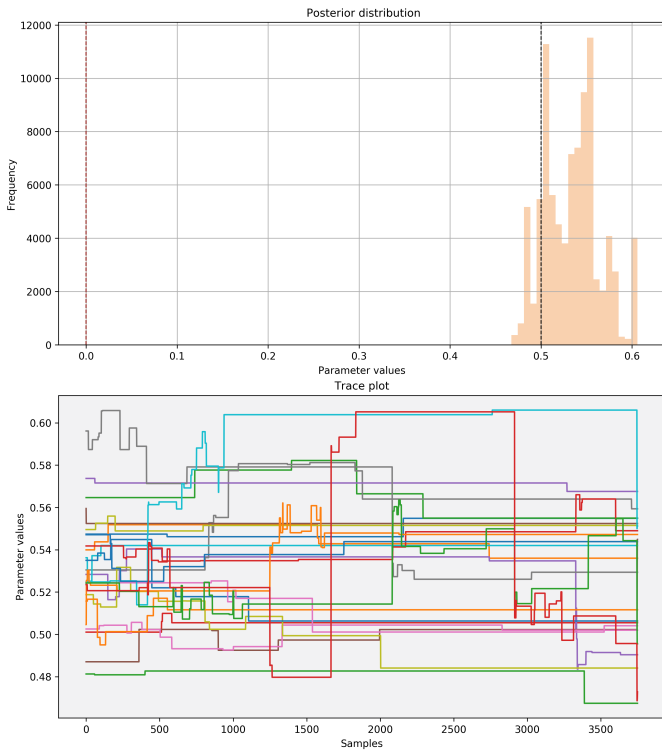


Figure 11: Typical posterior distribution (top panel) and replica traces (bottom panel) exploring the marine diffusion parameter-space for the CM-extended topography. In this model run 24 replicas are represented by the coloured lines. Parameter, c -marine, units are $m^2 a^{-1}$.

posterior distributions contained the true parameter. This is not surprising when one considers the highly irregular shape of the likelihood surface, as given in Figure 1[27]. Despite this variability in results the predictions were accurate which could be attributable to a multi-modal posterior. Multi-modal distribu-

tions are well known in Earth science problems in the literature (e.g. [63] and [64]). Multi-modality implies that there are several optimal values of the parameters where multiple combinations of the given parameters can plausibly predict or simulate the topography that closely resembles the synthetic or ground-truth topography [65].

Figure 13 shows the posterior distribution of the uplift parameter for the Mountain topography. In this case the chains found the true value early and did not stray far in their exploration, likely because the uplift parameter is not sensitive to the solution at the scales explored here (0.1 – 1.7 mm/a). The likelihood surface shown in Figure 15 suggests this, as rainfall increases and uplift decreases (with other parameters set to their true values) the likelihood remains high. Adjusting the temperature of the chains and swap ratios can help influence the exploration of the chains to fit the problem more appropriately. Yet here Figure 14 shows that the ground-truth and the PT-Bayelands predictions fit well, indicating that the explored space collectively for all parameters taken together was sufficient to match the data.

Furthermore, the experiments considered a fixed value for some parameters, such as rainfall, that can have varying effects given different regions and geological timescales. It is well known that climate change may affect rainfall with varying implications to the environment, and in this case the topography in terms of elevation via affecting erosion and sedimentation. Therefore, it would be reasonable to implement region- and time-dependent constraints for some parameters to fully take into account the effects of climate changes.

6. Conclusions and Future Work

We presented a computationally efficient implementation of multi-core parallel tempering for improving the computational time require to estimate parameters of the Bayeslands model. The proposed methodology provides a general systematic approach for uncertainty quantification of free parameters in basin and landscape dynamics models (Badlands). The results showed that the method not only reduces the computation time, but also provides a means to explore the parameter space in highly irregular multi-modal landscapes. This has been demonstrated by the results that show better posterior distributions of the parameters along with improvement in prediction accuracy of topography and sediment deposition.

Future work will extend the method for a larger number of parameters that includes spatio-temporal variations in rainfall and uplift for different timescales and regions. Moreover, for large-scale or continental-scale problems, it would be reasonable to implement further enhancements to the method for lowering the overall computational time. This could be done through surrogate-assisted models where at times the surrogate of Badlands implemented via machine learning evaluates the proposals. There is scope for real-world applications, that feature landscape evolution for geological timescales. Further, efficient gradient free proposals need to be constructed as the number of parameters and the complexity of the model increases.

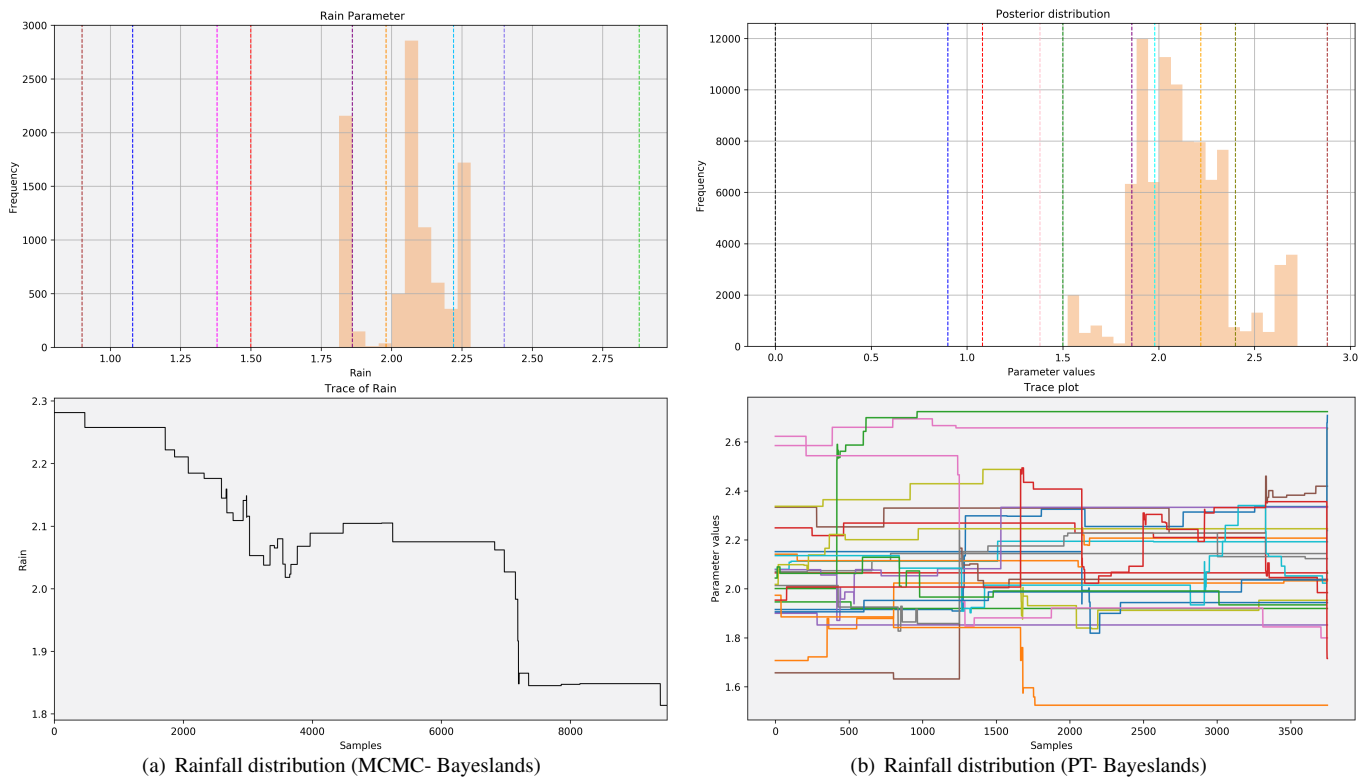


Figure 12: Comparison of PT-Bayeslands with MCMC-Bayeslands for the CM problem. Note that the vertical dashed lines in different colours shows sub-optimal true values or modes that correspond to the likelihood surface in Figure 1.

Acknowledgements

We would like to thank Danial Azam from School of Geoscience, the University of Sydney for providing technical assistance. We would also like to thank the Strategic Research Excellence Initiative (SREI) Grant from the University of Sydney. Furthermore, we would like to acknowledge the Artemis high performance computing infrastructure provided by Sydney Informatics Hub of the University of Sydney.

References

References

- [1] N. Flament, M. Gurnis, and R. D. Müller, "A review of observations and models of dynamic topography," *Lithosphere*, vol. 5, no. 2, pp. 189–210, 2013.
- [2] T. Coulthard, "Landscape evolution models: a software review," *Hydrological processes*, vol. 15, no. 1, pp. 165–173, 2001.
- [3] T. Salles and L. Hardiman, "Badlands: An open-source, flexible and parallel framework to study landscape dynamics," *Computers & Geosciences*, vol. 91, pp. 77–89, 2016.
- [4] T. Salles, N. Flament, and D. Müller, "Influence of mantle flow on the drainage of eastern australia since the jurassic period," *Geochemistry, Geophysics, Geosystems*, vol. 18, no. 1, pp. 280–305, 2017.
- [5] L. R. Scott and S. Zhang, "Finite element interpolation of nonsmooth functions satisfying boundary conditions," *Mathematics of Computation*, vol. 54, no. 190, pp. 483–493, 1990.
- [6] V. Godard, J. Lavé, and R. Cattin, "Numerical modelling of erosion processes in the himalayas of nepal: Effects of spatial variations of rock

- strength and precipitation," *Geological Society, London, Special Publications*, vol. 253, no. 1, pp. 341–358, 2006.
- [7] J. Rejman, R. Turski, and J. Paluszek, "Spatial and temporal variations in erodibility of loess soil," *Soil and Tillage Research*, vol. 46, no. 1-2, pp. 61–68, 1998.
- [8] G. Shafer, "Belief functions and parametric models," *Journal of the Royal Statistical Society. Series B (Methodological)*, pp. 322–352, 1982.
- [9] S. E. Fienberg *et al.*, "When did bayesian inference become 'bayesian'?" *Bayesian analysis*, vol. 1, no. 1, pp. 1–40, 2006.
- [10] N. L. Hjort, C. Holmes, P. Müller, and S. G. Walker, *Bayesian nonparametrics*. Cambridge University Press, 2010, vol. 28.
- [11] C. Robert and G. Casella, "A short history of markov chain monte carlo: Subjective recollections from incomplete data," *Statistical Science*, pp. 102–115, 2011.
- [12] K. Mosegaard and P. D. Vestergaard, "A simulated annealing approach to seismic model optimization with sparse prior information," *Geophysical Prospecting*, vol. 39, no. 5, pp. 599–611, 1991.
- [13] P. Rocca, M. Benedetti, M. Donelli, D. Franceschini, and A. Massa, "Evolutionary optimization as applied to inverse scattering problems," *Inverse Problems*, vol. 25, no. 12, p. 123003, 2009.
- [14] M. K. Sen and P. L. Stoffa, *Global optimization methods in geophysical inversion*. Cambridge University Press, 2013.
- [15] K. Gallagher, K. Charvin, S. Nielsen, M. Sambridge, and J. Stephenson, "Markov chain monte carlo (mcmc) sampling methods to determine optimal models, model resolution and model choice for earth science problems," *Marine and Petroleum Geology*, vol. 26, no. 4, pp. 525–535, 2009.
- [16] W. K. Hastings, "Monte carlo sampling methods using markov chains and their applications," *Biometrika*, vol. 57, no. 1, pp. 97–109, 1970.
- [17] N. Metropolis, A. W. Rosenbluth, M. N. Rosenbluth, A. H. Teller, and E. Teller, "Equation of state calculations by fast computing machines," *The journal of chemical physics*, vol. 21, no. 6, pp. 1087–1092, 1953.
- [18] A. E. Raftery and S. M. Lewis, "Implementing mcmc," *Markov chain Monte Carlo in practice*, pp. 115–130, 1996.

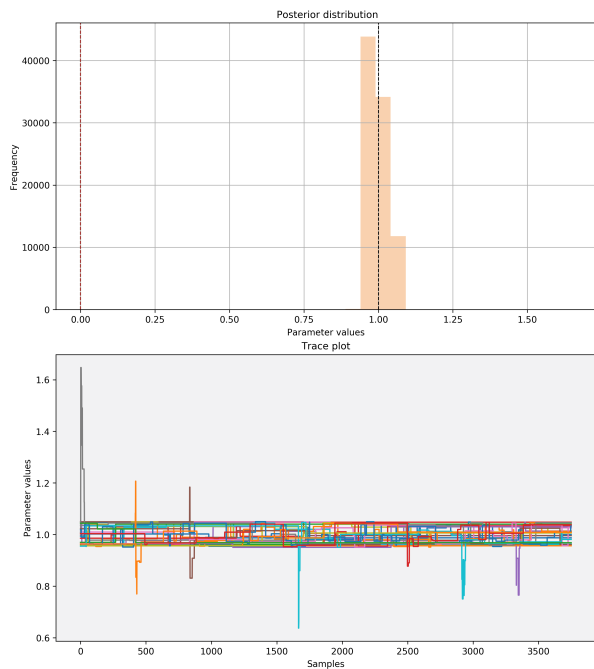
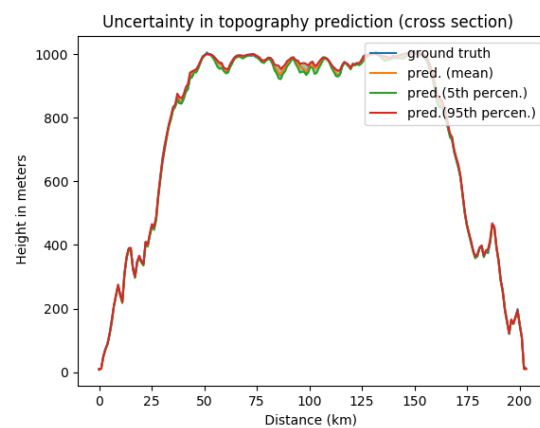
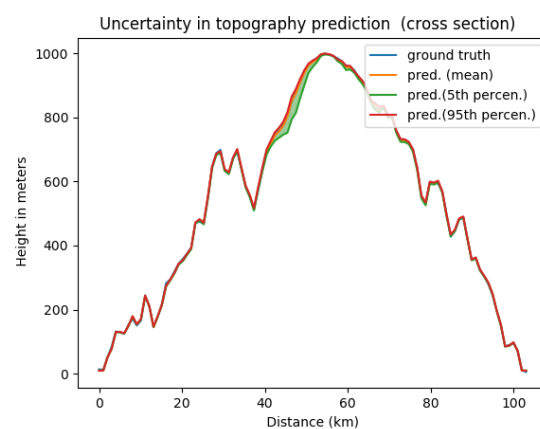


Figure 13: Posterior distribution (top panel) and replica traces (bottom panel) exploring the uplift parameter-space for the Mountain topography. The 24 replicas trace distribution are represented by the coloured lines. Parameter, uplift, units are $mm a^{-1}$.



(a) Cross-section along the x-axis.



(b) Cross-section along the y-axis

Figure 14: Typical topography for the evolved Mountain problem, comparing PT-Bayeslands predictions and the Badlands ground-truth. Result is for 24 replicas, 100,000 samples.

- [19] D. van Ravenzwaaij, P. Cassey, and S. D. Brown, “A simple introduction to markov chain monte-carlo sampling,” *Psychonomic bulletin & review*, pp. 1–12, 2016.
- [20] A. Malinverno, “Parsimonious bayesian markov chain monte carlo inversion in a nonlinear geophysical problem,” *Geophysical Journal International*, vol. 151, no. 3, pp. 675–688, 2002.
- [21] K. Mosegaard and A. Tarantola, “Monte carlo sampling of solutions to inverse problems,” *Journal of Geophysical Research: Solid Earth*, vol. 100, no. B7, pp. 12 431–12 447, 1995.
- [22] M. Sambridge and K. Mosegaard, “Monte carlo methods in geophysical inverse problems,” *Reviews of Geophysics*, vol. 40, no. 3, 2002.
- [23] M. Sambridge, “Geophysical inversion with a neighbourhood algorithm—ii. appraising the ensemble,” *Geophysical Journal International*, vol. 138, no. 3, pp. 727–746, 1999.
- [24] R. M. Neal *et al.*, “Mcmc using hamiltonian dynamics,” *Handbook of Markov Chain Monte Carlo*, vol. 2, no. 11, 2011.
- [25] M. D. Hoffman and A. Gelman, “The no-u-turn sampler: adaptively setting path lengths in hamiltonian monte carlo,” *Journal of Machine Learning Research*, vol. 15, no. 1, pp. 1593–1623, 2014.
- [26] M. Girolami and B. Calderhead, “Riemann manifold langevin and hamiltonian monte carlo methods,” *Journal of the Royal Statistical Society: Series B (Statistical Methodology)*, vol. 73, no. 2, pp. 123–214, 2011.
- [27] R. Chandra, D. Azam, D. Muller, T. Salles, and S. Cripps, “Bayeslands: A bayesian inference approach for parameter tuning for modelling basin and landscape dynamics via badlands,” *Computers and Geoscience*, pp. In-Review, 2018. [Online]. Available: <https://github.com/rohitash-chandra/research/blob/master/2018/BayesLands.pdf>
- [28] E. Marinari and G. Parisi, “Simulated tempering: a new monte carlo scheme,” *EPL (Europhysics Letters)*, vol. 19, no. 6, p. 451, 1992.
- [29] C. J. Geyer and E. A. Thompson, “Annealing markov chain monte carlo with applications to ancestral inference,” *Journal of the American Statistical Association*, vol. 90, no. 431, pp. 909–920, 1995.
- [30] H. Zhang, M. Liu, Y. Shi, D. A. Yuen, Z. Yan, and G. Liang, “Toward an automated parallel computing environment for geosciences,” *Physics of the Earth and Planetary Interiors*, vol. 163, no. 1–4, pp. 2–22, 2007.
- [31] J. A. Vrugt, B. O. Nualláin, B. A. Robinson, W. Bouten, S. C. Dekker, and

- P. M. Sloot, “Application of parallel computing to stochastic parameter estimation in environmental models,” *Computers & Geosciences*, vol. 32, no. 8, pp. 1139–1155, 2006.
- [32] K. Mills, G. Fox, and R. Heimbach, “Implementing an intervisibility analysis model on a parallel computing system,” *Computers & Geosciences*, vol. 18, no. 8, pp. 1047–1054, 1992.
- [33] K. X. Whipple and G. E. Tucker, “Implications of sediment-flux-dependent river incision models for landscape evolution,” *Journal of Geophysical Research: Solid Earth*, vol. 107, no. B2, pp. 1–20, 2002.
- [34] G. E. Tucker and G. R. Hancock, “Modelling landscape evolution,” *Earth Surface Processes and Landforms*, vol. 35, no. 1, pp. 28–50, 2010.
- [35] T. Salles and G. Duclaux, “Combined hillslope diffusion and sediment transport simulation applied to landscape dynamics modelling,” *Earth Surf. Process Landf.*, vol. 40, no. 6, p. 823–39, 2015.
- [36] B. Campforts, W. Schwanghart, and G. Govers, “Accurate simulation of transient landscape evolution by eliminating numerical diffusion: the ttem 1.0 model,” *Earth Surface Dynamics*, vol. 5, no. 1, pp. 47–66, 2017.
- [37] J. M. Adams, N. M. Gasparini, D. E. J. Hobbey, G. E. Tucker, E. W. H. Hutton, S. S. Nudurupati, and E. Istanbuluoglu, “The landlab v1.0 over-landflow component: a python tool for computing shallow-water flow across watersheds,” *Geoscientific Model Development*, vol. 10, no. 4, pp. 1645–1663, 2017.
- [38] A. D. Howard, W. E. Dietrich, and M. A. Seidl, “Modeling fluvial erosion on regional to continental scales,” *Journal of Geophysical Research:*

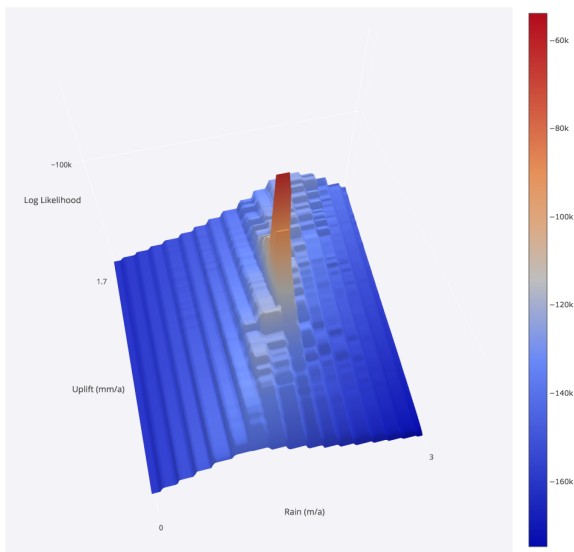


Figure 15: Likelihood surface of the Mountain topography for the rainfall and uplift parameters only.

- Solid Earth*, vol. 99, no. B7, pp. 13 971–13 986, 1994.
- [39] D. E. J. Hobley, H. D. Sinclair, S. M. Mudd, and P. A. Cowie, “Field calibration of sediment flux dependent river incision,” *Journal of Geophysical Research: Earth Surface*, vol. 116, no. F4, 2011.
- [40] T. Salles, “Badlands: A parallel basin and landscape dynamics model,” *SoftwareX*, vol. 5, pp. 195–202, 2016.
- [41] T. Salles, X. Ding, and G. Brocard, “pybadlands: A framework to simulate sediment transport, landscape dynamics and basin stratigraphic evolution through space and time,” *PLOS ONE*, vol. 13, pp. 1–24, 04 2018.
- [42] T. Salles, X. Ding, J. M. Webster, A. Vila-Concejo, G. Brocard, and J. Pall, “A unified framework for modelling sediment fate from source to sink and its interactions with reef systems over geological times,” *Scientific Reports*, vol. 8, no. 1, p. 5252, 2018.
- [43] S. Chib and E. Greenberg, “Understanding the metropolis-hastings algorithm,” *The American Statistician*, vol. 49, no. 4, pp. 327–335, 1995.
- [44] R. M. Neal, “Sampling from multimodal distributions using tempered transitions,” *Statistics and computing*, vol. 6, no. 4, pp. 353–366, 1996.
- [45] P. Baldi, “Gradient descent learning algorithm overview: A general dynamical systems perspective,” *IEEE Transactions on neural networks*, vol. 6, no. 1, pp. 182–195, 1995.
- [46] H. Strathmann, D. Sejdinovic, S. Livingstone, Z. Szabo, and A. Gretton, “Gradient-free hamiltonian monte carlo with efficient kernel exponential families,” in *Advances in Neural Information Processing Systems*, 2015, pp. 955–963.
- [47] A. Patriksson and D. van der Spoel, “A temperature predictor for parallel tempering simulations,” *Physical Chemistry Chemical Physics*, vol. 10, no. 15, pp. 2073–2077, 2008.
- [48] K. Hukushima and K. Nemoto, “Exchange monte carlo method and application to spin glass simulations,” *Journal of the Physical Society of Japan*, vol. 65, no. 6, pp. 1604–1608, 1996.
- [49] U. H. Hansmann, “Parallel tempering algorithm for conformational studies of biological molecules,” *Chemical Physics Letters*, vol. 281, no. 1–3, pp. 140–150, 1997.
- [50] M. K. Sen and P. L. Stoffa, “Bayesian inference, gibbs’ sampler and uncertainty estimation in geophysical inversion,” *Geophysical Prospecting*, vol. 44, no. 2, pp. 313–350, 1996.
- [51] M. Maraschini and S. Foti, “A monte carlo multimodal inversion of surface waves,” *Geophysical Journal International*, vol. 182, no. 3, pp. 1557–1566, 2010.
- [52] A. Kone and D. A. Kofke, “Selection of temperature intervals for parallel-tempering simulations,” *The Journal of chemical physics*, vol. 122, no. 20, p. 206101, 2005.
- [53] F. Calvo, “All-exchanges parallel tempering,” *The Journal of chemical physics*, vol. 123, no. 12, p. 124106, 2005.
- [54] B. Miasojedow, E. Moulines, and M. Vihola, “An adaptive parallel tempering algorithm,” *Journal of Computational and Graphical Statistics*, vol. 22, no. 3, pp. 649–664, 2013.
- [55] M. Sambridge, “A parallel tempering algorithm for probabilistic sampling and multimodal optimization,” *Geophysical Journal International*, vol. 196, no. 1, pp. 357–374, 2013.
- [56] L. Lafort, “On interprocess communication,” *Distributed computing*, vol. 1, no. 2, pp. 86–101, 1986.
- [57] Y. Li, M. Mascagni, and A. Gorin, “A decentralized parallel implementation for parallel tempering algorithm,” *Parallel Computing*, vol. 35, no. 5, pp. 269 – 283, 2009.
- [58] K. Karimi, N. Dickson, and F. Hamze, “High-performance physics simulations using multi-core cpus and gpgpus in a volunteer computing context,” *The International Journal of High Performance Computing Applications*, vol. 25, no. 1, pp. 61–69, 2011.
- [59] G. Mingas, L. Bottolo, and C.-S. Bouganis, “Particle mcmc algorithms and architectures for accelerating inference in state-space models,” *International Journal of Approximate Reasoning*, vol. 83, pp. 413–433, 2017.
- [60] A. Reid, E. V. Bonilla, L. McCalman, T. Rawling, and F. Ramos, “Bayesian joint inversions for the exploration of Earth resources,” in *IJ-CAI*, 2013, pp. 2877–2884.
- [61] H. Jeffreys, “An invariant form for the prior probability in estimation problems,” *Proceedings of the Royal Society of London. Series A, Mathematical and Physical Sciences*, pp. 453–461, 1946.
- [62] N. Singh, L.-M. Browne, and R. Butler, “Parallel astronomical data processing with python: Recipes for multicore machines,” *Astronomy and Computing*, vol. 2, pp. 1–10, 2013.
- [63] M. Dalla Mura, S. Prasad, F. Pacifici, P. Gamba, J. Chanussot, and J. A. Benediktsson, “Challenges and opportunities of multimodality and data fusion in remote sensing,” *Proceedings of the IEEE*, vol. 103, no. 9, pp. 1585–1601, 2015.
- [64] A. Beskos, M. Girolami, S. Lan, P. E. Farrell, and A. M. Stuart, “Geometric mcmc for infinite-dimensional inverse problems,” *Journal of Computational Physics*, vol. 335, pp. 327–351, 2017.
- [65] T. A. Cross and M. A. Lessenger, “Construction and application of a stratigraphic inverse model,” in *Numerical Experiments in Stratigraphy: Recent Advances in Stratigraphic and Sedimentologic Computer Simulations*, J. Harbaugh, W. Watney, E. Rankey, R. Slingerland, R. Goldstein, and E. Franseen, Eds. Special publications of Society for Sedimentary Geology, 1999, ch. 62, pp. 69–83.